

Tolerance checkpoint bypass permits emergence of pathogenic T cells to neuromyelitis optica autoantigen aquaporin-4

Sharon A. Sagan^{a,b,1}, Ryan C. Winger^{a,b,1}, Andrés Cruz-Herranz^{a,1}, Patricia A. Nelson^{a,b}, Sarah Hagberg^{a,b,c}, Corey N. Miller^{b,d}, Collin M. Spencer^{a,b}, Peggy P. Ho^e, Jeffrey L. Bennett^{f,g}, Michael Levy^h, Marc H. Levin^c, Alan S. Verkman^{i,j}, Lawrence Steinman^{e,2}, Ari J. Green^a, Mark S. Anderson^{b,d}, Raymond A. Sobel^k, and Scott S. Zamvil^{a,b,2}

^aDepartment of Neurology, University of California, San Francisco, CA 94143; ^bProgram in Immunology, University of California, San Francisco, CA 94143; ^cDepartment of Ophthalmology, University of California, San Francisco, CA 94143; ^dDiabetes Center, University of California, San Francisco, CA 94143; ^eDepartment of Neurology and Neurological Sciences, Stanford University, Stanford, CA 94305; ^fDepartment of Neurology, Neuroscience Program, University of Colorado, Denver, CO 80045; ^gDepartment of Ophthalmology, University of Colorado, Denver, CO 80045; ^hDepartment of Neurology, Johns Hopkins University, Baltimore, MD 21287; ⁱDepartment of Medicine, University of California, San Francisco, CA 94143; ^jDepartment of Physiology, University of California, San Francisco, CA 94143; and ^kDepartment of Pathology, Stanford University, Stanford, CA 94305

Contributed by Lawrence Steinman, November 10, 2016 (sent for review October 26, 2016; reviewed by Nathan Karin and Howard L. Weiner)

Aquaporin-4 (AQP4)-specific T cells are expanded in neuromyelitis optica (NMO) patients and exhibit Th17 polarization. However, their pathogenic role in CNS autoimmune inflammatory disease is unclear. Although multiple AQP4 T-cell epitopes have been identified in WT C57BL/6 mice, we observed that neither immunization with those determinants nor transfer of donor T cells targeting them caused CNS autoimmune disease in recipient mice. In contrast, robust proliferation was observed following immunization of AQP4-deficient (AQP4^{-/-}) mice with AQP4 peptide (p) 135–153 or p201–220, peptides predicted to contain I-A^b-restricted T-cell epitopes but not identified in WT mice. In comparison with WT mice, AQP4^{-/-} mice used unique T-cell receptor repertoires for recognition of these two AQP4 epitopes. Donor T cells specific for either determinant from AQP4^{-/-}, but not WT, mice induced paralysis in recipient WT and B-cell-deficient mice. AQP4-specific Th17-polarized cells induced more severe disease than Th1-polarized cells. Clinical signs were associated with opticospinal infiltrates of T cells and monocytes. Fluorescent-labeled donor T cells were detected in CNS lesions. Visual system involvement was evident by changes in optical coherence tomography. Fine mapping of AQP4 p201–220 and p135–153 epitopes identified peptides within p201–220 but not p135–153, which induced clinical disease in 40% of WT mice by direct immunization. Our results provide a foundation to evaluate how AQP4-specific T cells contribute to AQP4-targeted CNS autoimmunity (ATCA) and suggest that pathogenic AQP4-specific T-cell responses are normally restrained by central tolerance, which may be relevant to understanding development of AQP4-reactive T cells in NMO.

neuromyelitis optica | aquaporin-4 | T-cell receptor | tolerance | ENMO

Neuromyelitis optica (NMO) is a rare, disabling, and sometimes fatal CNS autoimmune inflammatory demyelinating disease that causes attacks of paralysis and visual loss (1). Immunologic, epidemiologic, and pathologic evidence suggests T cells have an important role in the etiology of NMO (1–3). Pathogenic aquaporin-4 (AQP4)-specific antibodies in NMO serum are predominantly IgG1, a T-cell-dependent IgG subclass (4), and T-cell-mediated CNS inflammation permits CNS entry of those antibodies (5, 6). NMO susceptibility is associated with allelic MHC II genes, in particular HLA-DR17 (DRB1*0301) in certain populations (7). AQP4-specific T cells have been identified in patients (8, 9), and T cells specific for dominant AQP4 epitopes exhibit Th17 polarization (8). It is therefore important to understand factors that control development and regulate the expression of AQP4-specific T cells in NMO.

One cannot feasibly test whether AQP4-reactive T cells participate directly in CNS inflammation in NMO patients. Animal

models can permit in vivo evaluation of the role of AQP4-specific T cells in CNS autoimmunity. Although multiple AQP4 T-cell epitopes have been identified in WT mice and rats (10–13), attempts to create AQP4-targeted experimental NMO (“ENMO”) with clinical manifestations of CNS autoimmune disease by either direct immunization of those determinants or adoptive transfer of T cells targeting them have been unsuccessful (11–13).

Recently, it was observed that immunization of AQP4-deficient (AQP4^{-/-}) mice with AQP4 peptide (p) 135–153 elicited T-cell proliferation and that those T cells induced mild clinical disease in 70% of recipient WT mice (14). Here, we evaluated T-cell reactivity to AQP4 in C57BL/6 AQP4^{-/-} and WT mice and identified two pathogenic AQP4 T-cell determinants, one within AQP4 residues 135–153 and one in 201–220. Both determinants were predicted to bind MHC II (I-A^b) avidly and elicit I-A^b-restricted AQP4-specific CD4⁺ T-cell responses (15), yet only T cells from AQP4^{-/-}, but not WT, mice proliferated robustly to those epitopes. Hyperproliferation was AQP4-specific, as immunization with a

Significance

Neuromyelitis optica (NMO) is a CNS autoimmune demyelinating disease involving aquaporin-4 (AQP4)-specific IgG1, a T-cell-dependent antibody subclass. The role of T cells in NMO is unclear. We evaluated AQP4-specific T cells in WT and AQP4^{-/-} mice. AQP4 epitopes identified in WT mice were not pathogenic. AQP4 peptide (p) 135–153 and p201–220 elicited robust T-cell responses in AQP4^{-/-} but not WT, mice. T-cell receptor repertoire utilization for these determinants in AQP4^{-/-} mice was unique. Donor AQP4^{-/-} p135–153- or p201–220-specific Th17 cells entered the CNS of recipient WT mice and induced CNS autoimmunity. Our findings indicate pathogenic AQP4-specific T cells are normally restrained by central tolerance, which could be relevant to understanding the origin of pathogenic T cells in NMO.

Author contributions: S.A.S., R.C.W., A.C.-H., P.A.N., P.P.H., L.S., R.A.S., and S.S.Z. designed research; S.A.S., R.C.W., A.C.-H., P.A.N., S.H., P.P.H., L.S., and R.A.S. performed research; A.S.V. contributed new reagents/analytic tools; S.A.S., R.C.W., A.C.-H., P.A.N., C.N.M., C.M.S., P.P.H., J.L.B., M.L., M.H.L., A.J.G., M.S.A., and R.A.S. analyzed data; and S.A.S., R.C.W., A.C.-H., L.S., R.A.S., and S.S.Z. wrote the paper.

Reviewers: N.K., Israel Institute of Technology; and H.L.W., Brigham and Women’s Hospital.

The authors declare no conflict of interest.

Freely available online through the PNAS open access option.

¹S.A.S., R.C.W., and A.C.-H. contributed equally to this work.

²To whom correspondence may be addressed. Email: zamvil@ucsf.neuroimmunol.org or steinman@stanford.edu.

This article contains supporting information online at www.pnas.org/lookup/suppl/doi:10.1073/pnas.1617859114/-DCSupplemental.

myelin oligodendrocyte glycoprotein (MOG) peptide induced equal proliferation in AQP4^{-/-} and WT mice. Compared with T cells in WT mice, T-cell and T-cell receptor (TCR) repertoires used by AQP4-specific T cells in AQP4^{-/-} mice were unique. Transfer of either AQP4 p135–153- or p201–220-specific Th17-polarized cells from AQP4^{-/-} donor mice consistently induced paralysis and histologic CNS autoimmune disease in nearly 100% of naïve recipient WT mice. Peptides within AQP4 201–220 but not 135–153 were identified that induced clinical disease in WT mice by direct immunization. AQP4-specific T-cell-mediated clinical disease was associated with opticospinal infiltrates of T cells, B cells, and monocytes, and dynamic visual system involvement was also evident by changes in optical coherence tomography (OCT). Our observations indicate that the pathogenic AQP4-specific T-cell repertoire is controlled by negative selection.

Results

AQP4-Specific T Cells from WT and AQP4^{-/-} Mice Use Distinct T-Cell Repertoires. Previously, we identified multiple immunodominant AQP4 T-cell epitopes in WT C57BL/6 and SJL/J mice (10). Here, we examined whether those T-cell determinants could induce CNS autoimmune disease, either by direct immunization or by adoptive transfer of Th1- or Th17-polarized T cells targeting those epitopes (Table S1). Neither clinical nor histological signs of CNS autoimmune disease were observed in either strain following direct immunization of those AQP4 determinants or in naïve mice that received donor AQP4-specific T cells. Histologic signs of CNS disease were observed inconsistently in recipient SJL/J mice that had received prior low-dose whole-body irradiation but not in mice given *Bordetella pertussis* toxin (Table S2). RAG2^{-/-} mice, devoid of mature T cells and B cells, can be more susceptible to EAE-induced myelin-specific T cells (16). SJL/J AQP4 p23–35-specific T cells were also incapable of causing clinical disease in syngeneic SJL/J RAG2^{-/-} mice. Thus, AQP4 T-cell determinants initially identified by screening WT mice did not elicit clinical signs of CNS pathology.

Working with C57BL/6 AQP4^{-/-} mice to generate antibodies to the AQP4 extracellular C loop, p135–153, Levy and colleagues (14) observed that this peptide induced T-cell proliferation and that donor AQP4^{-/-} proinflammatory AQP4 p135–153-specific T cells caused mild paralysis in ~70% of WT recipient mice. They did not evaluate the response to AQP4 p135–153 in WT mice. Of interest, p135–153 is located within a region of AQP4 that is predicted to bind I-A^b avidly and elicit T-cell responses according to the immune epitope database (IEDB), an *in silico* method for predicting determinants with proteins that bind allele-specific MHC molecules, which is based on existing quantitative MHC-peptide binding affinities for known T-cell epitopes of protein antigens (Fig. 1A) (10, 15). We observed that AQP4 p135–153 induced robust proliferation in C57BL/6 AQP4^{-/-} mice but not in WT mice (Fig. 1B). AQP4 p201–220, which is also predicted to contain an MHC II (I-A^b)-restricted T-cell epitope by IEDB, induced much stronger proliferation in AQP4^{-/-} than WT mice. This observation suggested that proliferation to these determinants in AQP4^{-/-} mice reflected loss of central tolerance to AQP4. Indeed, proliferation induced by immunization with MOG p35–55 was similar in AQP4^{-/-} and WT mice, confirming that “hyperproliferation” to either AQP4 p135–153 or p201–220 was AQP4-specific. Interestingly, p24–35, p91–110, and p261–280, immunogenic determinants identified in WT C57BL/6 mice (10), induced modest but similar proliferation in AQP4^{-/-} and WT mice.

To evaluate the possibility that T-cell hyperreactivity to AQP4 p135–153 and p201–220 in AQP4^{-/-} mice could be attributed to a loss of negative selection, we examined whether AQP4 deficiency influenced TCR gene use. There were no differences in the naïve TCR V β repertoire in AQP4^{-/-} compared with WT mice (Fig. 2A). However, TCR V β utilization by T cells targeting those two determinants in AQP4^{-/-} and WT mice was distinct. The most commonly used TCR V β by p135–153-specific T cells from AQP4^{-/-} mice was V β 3 and reflected nearly a threefold increase relative to use by WT T cells. There was a sixfold expansion of V β 6 by AQP4 p201–220-specific T cells in AQP4^{-/-} mice but no

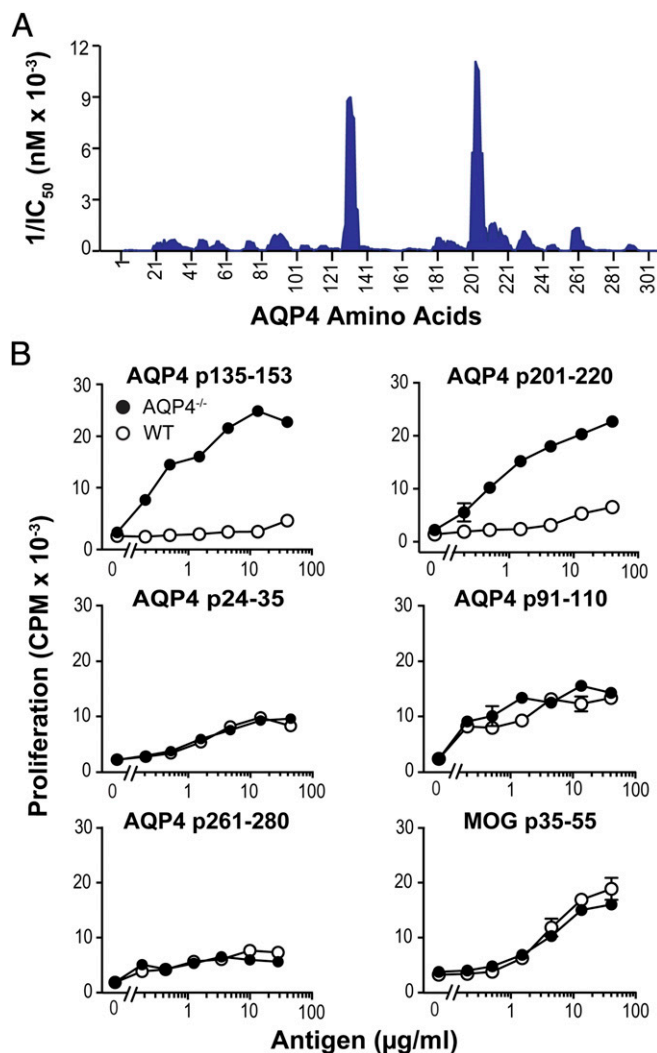


Fig. 1. Two AQP4 determinants elicit vigorous T-cell proliferation in AQP4^{-/-} mice. (A) IEDB, an *in silico* method for predicting determinants within proteins that bind MHC alleles, was used to identify amino acid sequences within AQP4 anticipated to bind I-A^b for recognition by CD4⁺ T cells (15). 1/IC₅₀ is plotted against the first amino acid for each overlapping AQP4 15 mer. Peaks correspond to increased predicted binding affinity. (B) Mice were immunized s.c. with the indicated peptides in CFA. Proliferation was measured by ³H-thymidine incorporation (mean ± SEM, representative of five experiments).

significant increase in use of this V β by p201–220-specific T cells in WT mice. The TCR V β repertoire to MOG p35–55, a control, was similar in AQP4^{-/-} and WT mice. We did not detect significant differences in frequencies of CD4⁺CD25⁺Foxp3⁺ Treg, Th1, Th17, CD11b⁺, CD11b⁺Ly6G⁺, or CD11c⁺ dendritic cells (DCs) between naïve AQP4^{-/-} and WT mice in secondary lymphoid tissue (Fig. 2B–D). No differences in leukocyte populations or apoptotic (annexin V⁺) cells were detected between AQP4-primed AQP4^{-/-} and WT mice (Fig. S1). Further, we did not detect significant differences in percentages of Th1 or Th17 cells from WT or AQP4^{-/-} mice after immunization with pathogenic or nonpathogenic AQP4 peptides in CFA alone. Collectively, our results indicate that AQP4 deficiency bypassed a tolerance checkpoint in AQP4-specific T-cell repertoire selection.

AQP4-Specific T Cells from AQP4^{-/-} Mice Induce Clinical and Histologic Opticospinal Inflammatory Disease in WT Mice. Proinflammatory AQP4-specific T cells from AQP4^{-/-} mice were tested for their capability to induce clinical CNS autoimmune disease. Initially, we evaluated

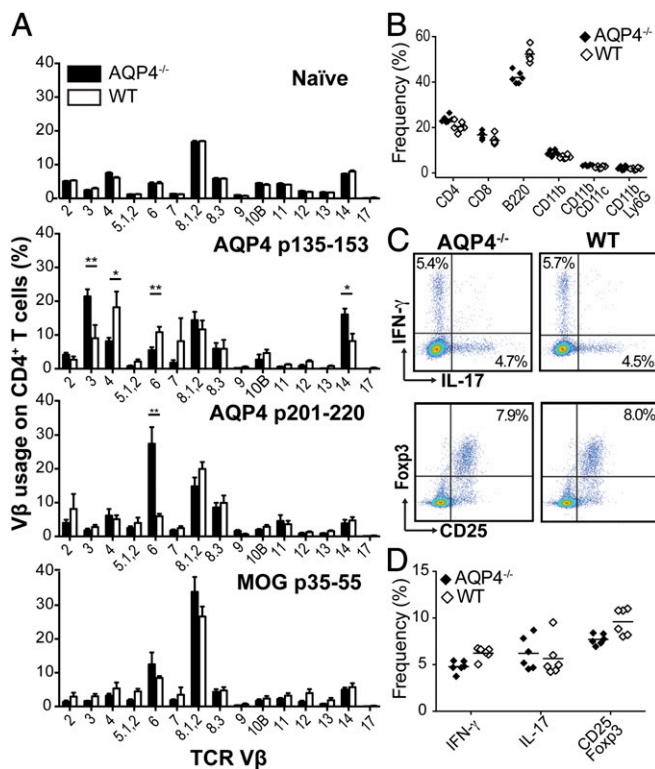


Fig. 2. TCR repertoire utilization by AQP4-specific T cells from AQP4^{-/-} mice is distinct. (A) AQP4^{-/-} and WT mice were immunized with the indicated peptides. TCR Vβ utilization was analyzed by FACS (mean ± SEM, n = 5, *P < 0.05, **P < 0.01). Frequencies of peripheral leukocyte subsets (B) and Th1, Th17, and CD4⁺CD25⁺Foxp3⁺ Treg cells (C and D) in naive AQP4^{-/-} and WT mice (n = 6) are shown. (C) Representative FACS plots are shown for T-cell subsets.

Th17-polarized AQP4-reactive T cells, as evidence suggests that AQP4-specific Th17 cells participate in NMO pathogenesis (Fig. S2) (8, 17, 18). AQP4 p135–153-specific or p201–220-specific Th17 cells induced paralysis in nearly 100% of recipient WT mice tested (Fig. 3A, Table 1, and Movie S1). Those AQP4-specific T cells did not induce clinical or histological disease in AQP4^{-/-} mice, confirming autoantigen specificity (Table 1). Several mice developed

paraplegia, and mean maximal clinical severity was similar to EAE induced by MOG-specific T cells. However, onset of paralysis induced by AQP4 p135–153-specific or p201–220-specific T cells often occurred earlier, and in contrast with EAE induced by WT MOG-specific T cells, recovery was complete. We also compared the pathogenic capability of Th1- and Th17-polarized AQP4-specific T cells. Th17-polarized AQP4 p135–153-specific or p201–220-specific T cells consistently induced more severe clinical disease (Fig. 3B and Table 1). Further, fluorescently labeled donor Th17-polarized AQP4 p201–220-specific T cells were identified within CNS parenchymal inflammatory lesions (Fig. 3C). Development of AQP4-targeted CNS autoimmune (ATCA) disease was B-cell-independent, as AQP4 p201–220-specific T cells induced clinical disease in B-cell-deficient (J_HT) recipients with equal severity to WT recipients (Table 1).

Clinical disease was associated with histologic CNS pathology in Th17-polarized AQP4 p135–153-specific and p201–220-specific T-cell recipients (Fig. 4A). CNS inflammatory infiltrates were detected in the parenchyma but were more numerous in the meninges (Table 1 and Table S3). CNS infiltrates consisted of T cells and B cells in meninges and parenchyma, and reactive monocytes/microglia in the parenchyma. Neutrophils and eosinophils, which are characteristic of NMO lesions, were not detected in the infiltrates. Axonal integrity was generally preserved in AQP4-induced CNS autoimmunity, whereas disease induced by MOG-specific Th17 cells resulted in greater axonal disruption and loss in the spinal cord (Fig. 4A). Optic nerve inflammation was also evident and characterized primarily as a perineuritis in AQP4 peptide-specific T-cell recipients, whereas MOG-specific T cells induced severe optic neuritis (Fig. 4B). Although AQP4 is expressed in kidney and skeletal muscle (19), histopathologic abnormalities were not detected in these organs in any mice (Table S4).

OCT Can Be Used to Monitor AQP4-Specific T-Cell-Mediated Optic Nerve Inflammation. Damage to optic nerves in NMO is associated with retinal injury, including thinning of the inner retinal layers (IRLs) and axonal damage (20). Therefore, we also evaluated optic nerve involvement in recipients of encephalitogenic Th17-polarized AQP4-specific T cells by serial OCT. Optic nerve inflammation, indicated by swelling and increased IRL thickness, was detected and corresponded to the clinical disease course (Fig. 5A), with near complete return of IRL thickness to baseline upon recovery. Retinal whole-mount staining demonstrated preservation of retinal ganglion cells (RGCs) (Fig. 5B and C). In contrast, mice that received MOG-specific T cells exhibited persistent clinical disease, which was associated with progressive IRL thinning and loss of RGCs.

Table 1. Donor AQP4-primed T cells from AQP4^{-/-} mice induce clinical and histologic CNS autoimmunity in WT and B-cell-deficient mice

Donor T cells	Polarization*	Recipients	Incidence	Onset, d [†]	Mean maximal clinical score [†]	Mean number of foci (±SEM) [†]		
						Meninges	Parenchyma	Total
AQP4 p135–153	Th1	WT	8/9	7.8 (±0.5)	1.5 (±0.3)	25 (±9)	12 (±2)	37 (±10)
	Th17	WT	19/19	8.3 (±0.3)	2.5 (±0.2)	101 (±18)	38 (±10)	139 (±19)
	Th17	AQP4 ^{-/-}	0/4	—	—	0	0	0
AQP4 p201–220	Th1	WT	6/8	8.0 (±0.3)	1.3 (±0.2)	55 (±15)	17 (±5)	72 (±19)
	Th17	WT	21/23	7.5 (±0.3)	2.5 (±0.1)	135 (±15)	82 (±17)	206 (±28)
	Th17	J _H T	6/7	5.8 (±0.3)	2.3 (±0.1)	101 (±30)	53 (±20)	154 (±51)
	Th17	AQP4 ^{-/-}	0/4	—	—	0	0	0
AQP4 p24–35	Th17	WT	0/4	—	0	0	0	0
AQP4 p91–110	Th17	WT	0/4	—	0	0	0	0
AQP4 p261–280	Th17	WT	0/5	—	0	0	0	0
MOG p35–55	Th1	WT	21/23	8.2 (±0.2)	3.1 (±0.1)	115 (±10)	101 (±21)	216 (±11)
	Th17	WT	25/28	8.2 (±0.4)	3.4 (±0.2)	151 (±20)	163 (±13)	314 (±33)
	Th17	AQP4 ^{-/-}	3/3	8.3 (±0.3)	2.8 (±0.3)	162 (±20)	174 (±29)	336 (±50)

*Donor T cells (2 × 10⁷), polarized to Th1 or Th17, were administered i.v. to recipient mice.

[†]All values are shown as mean (± SEM); n = 5 per group unless otherwise indicated.

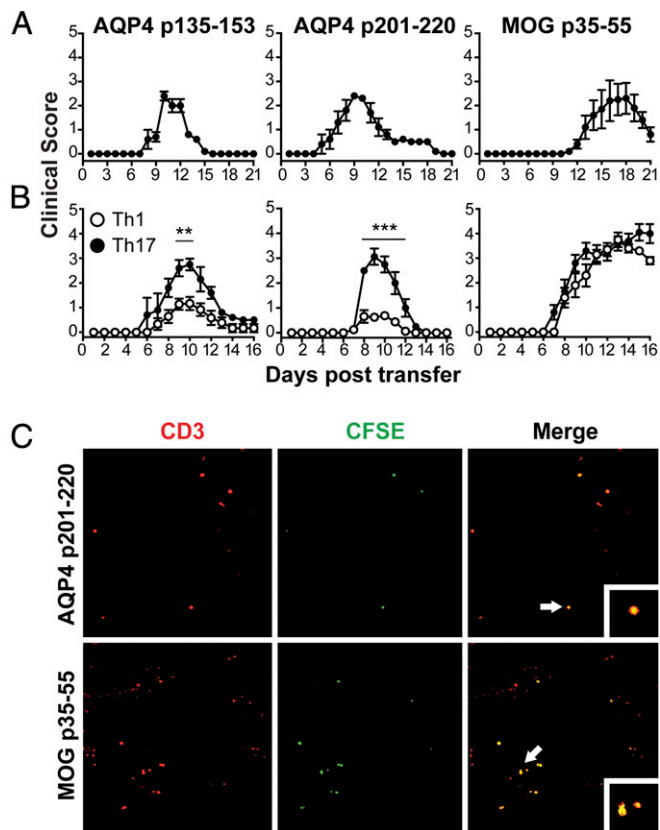


Fig. 3. Th17-polarized AQP4-specific T cells from AQP4^{-/-} mice induce paralysis in WT recipient mice. (A) Th17-polarized AQP4 p135–153 or p201–220-specific T cells from AQP4^{-/-} mice were transferred into WT recipients. Th17-polarized MOG-specific T cells served as a positive control. Results are representative of eight experiments ($n = 5$ per group). (B) Donor AQP4^{-/-} Th1- and Th17-polarized AQP4 p135–153 or p201–220-specific T cells were compared for induction of disease in WT recipient mice. In parallel, MOG p35–55-specific Th1- and Th17-polarized T cells were examined for EAE induction. Results are representative of three experiments ($n = 5$ per group). Mean clinical scores (\pm SEM) are shown in A and B (** $P < 0.01$, *** $P < 0.001$). (C) Confocal images (10 \times) of CD3⁺ T cells (red) and CFSE-labeled donor T cells (green) in the CNS parenchyma of recipient WT mice at peak disease. Arrows and *Insets* indicate CFSE⁺ CD3⁺ T-cell infiltrates (yellow). Results are representative of three mice per group.

Delineating T-Cell Specificity for Pathogenic AQP4 Epitopes. In general, antigen-specific MHC II-restricted CD4⁺ T cells recognize peptide fragments of 11–15 aa (21). Therefore, we evaluated AQP4 p135–153-specific and p201–220-specific T cells for recognition of truncated peptides. T cells from AQP4 p135–153-primed mice proliferated more efficiently (i.e., heteroclitic) to p131–150 but did not recognize p139–153 (Fig. 6A). T cells from AQP4 p131–150-primed mice proliferated to p131–150, p133–147, p133–149, and p135–149. Adoptive transfer of p135–149-specific T cells from AQP4^{-/-} mice caused clinical disease in WT mice, confirming encephalogenicity (Table S5). Immunization with the parent p135–153 or truncated p133–147 did not induce clinical disease (Fig. 6C).

T cells from AQP4^{-/-} mice primed with AQP4 p201–220 showed robust proliferation to p201–215; gave a partial response to p202–215, p204–215, and p205–215; and did not respond to p201–213 (Fig. 6B). AQP4 p201–215-specific T cells from AQP4^{-/-} mice induced disease in WT recipient mice (Table S5). Of particular interest, immunization of WT mice with p201–215 or p201–220 caused CNS autoimmune disease in some of the mice tested (Fig. 6C). The graph showing mean disease scores suggests p201–215 and p201–220 induced less severe disease but is not an accurate reflection, as mice either did not develop clinical disease or they developed paraparesis (Fig. 6D).

Discussion

Substantial evidence indicates that AQP4-specific Th17 cells participate in the pathogenesis of NMO (8, 17, 18). Despite observations that CNS inflammation induced by myelin-specific T cells facilitates entry of pathogenic AQP4-targeted antibodies (5, 6), most attempts to generate a model of clinical and histologic CNS autoimmune disease initiated by AQP4-specific T cells have proven unsuccessful (11–13). Here, we examined AQP4-specific T-cell responses in AQP4^{-/-} and WT mice in parallel. Proinflammatory T cells that recognized AQP4 epitopes initially identified from analysis of WT mice (10) were not pathogenic. In contrast, we have demonstrated that two distinct AQP4 determinants induce vigorous T-cell responses in AQP4^{-/-} mice and that those T cells are capable of causing both clinical and histologic CNS autoimmune disease in WT (i.e., AQP4⁺) mice or B-cell-deficient mice. AQP4-specific Th17 cells induced more severe clinical disease than Th1 cells, consistent with observations suggesting that NMO is an IL-17-mediated disease. Donor AQP4-specific Th17 cells were identified within CNS infiltrates, and despite known expression of AQP4 in other organs (e.g., muscle and kidney) (19), AQP4-targeted T-cell-mediated inflammation was selective for the CNS. Optic nerve inflammation was evident and, as occurs in NMO (22), by AQP4-reactive T cells was frequently as severe as EAE induced by WT MOG-specific T cells, recovery was the norm, and unlike EAE induced by MOG-specific T cells, pathogenic AQP4-specific T cells did not cause axonal loss in the spinal cord or loss of RGCs.

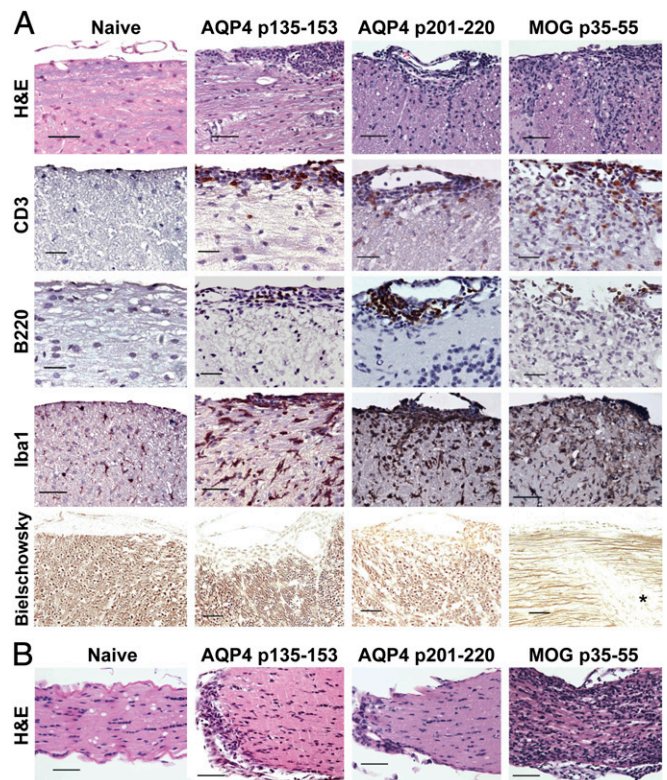


Fig. 4. AQP4-specific T cells from AQP4^{-/-} mice induce CNS inflammation in WT mice. Donor AQP4 p135–153- and p201–220-primed Th17 cells from AQP4^{-/-} mice were adoptively transferred to WT recipient mice. Donor MOG p35–55-specific Th17-polarized cells were examined in parallel. Mice were killed on day 10 and evaluated for histologic evidence of inflammation in (A) spinal cord and (B) optic nerve. Tissues were stained by H&E/LFB to evaluate inflammation and demyelination, respectively. CD3 T cells, B220 (CD45R) B cells, and Iba1⁺ monocyte/microglia were identified in CNS infiltrates by immunohistochemistry. Bielschowsky silver stain shows axonal loss (*). Results are representative of five mice per group. (Scale bar, 30 μ m.)

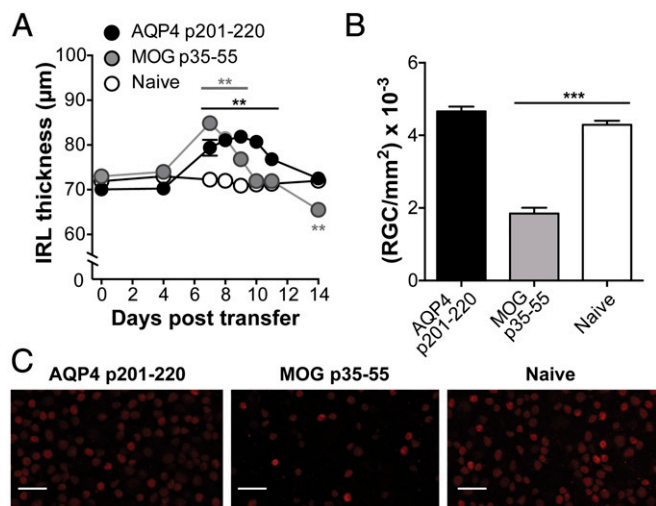


Fig. 5. Evaluation of AQP4-specific T-cell-mediated optic nerve (ON) inflammation by OCT. ON inflammation in WT recipient mice was induced by Th17-polarized AQP4 p201–220-specific or MOG-specific T cells and monitored by OCT. (A) IRL thickness was measured (mean \pm SEM). Statistics indicate a comparison with naive control (** $P < 0.01$). (B) Brn3a staining of RGCs on whole mounts and quantified as RGC/mm² (mean \pm SEM). Results in A and B are representative of three experiments (five mice per group). (C) Representative 20 \times confocal images showing RGC cell density in each group. (Scale bar, 30 μ m.)

Our observations that AQP4-specific Th17 cells from AQP4^{-/-} mice are capable of causing severe clinical CNS autoimmune disease, which is then followed by recovery, indicate that the T-cell immune response to AQP4, an autoantigen that is expressed ubiquitously, is normally regulated by stringent mechanisms of central and peripheral tolerance. These findings may be relevant to understanding development and maintenance of pathogenic AQP4-specific T cells in NMO.

Identification of robust proliferation to AQP4 p135–153 or p201–220 in AQP4^{-/-}, but not WT, mice suggests T-cell responses to those pathogenic AQP4 epitopes may be controlled by thymic negative selection. Indeed, the TCR repertoires used by the two pathogenic AQP4 T-cell epitopes in AQP4^{-/-} and WT mice were distinct, an observation that did not apply to a nonpathogenic AQP4 epitope or a control antigen (Fig. 2). Further, no differences in peripheral proinflammatory, regulatory, or apoptotic T cells were detected in secondary lymphoid tissue between AQP4-immunized AQP4^{-/-} and WT mice (Fig. S1). It is striking that IEDB predicted that only two regions of AQP4 bind I-A^b with high affinity, which correspond to the two pathogenic I-A^b-restricted AQP4-specific T-cell determinants identified in this report. This raises the possibility that T cells specific for those predicted high-avidity I-A^b-associated AQP4 determinants are subject to clonal deletion. Indeed, AQP4 protein is expressed in the thymus (23). Two distinct transcription factors, the autoimmune regulator (*Aire*) and *Fezf2*, are expressed by medullary thymic epithelial cells (mTECs) and control negative T-cell selection to the majority of tissue-specific antigens (24, 25). Although some data suggest that AQP4 expression by mTECs may be *Aire*-dependent (24, 26, 27), other evidence indicates that AQP4 expression may be *Fezf2*-dependent (25). Our findings that 40% of the WT mice immunized with AQP4 p201–220 or p201–215 but none of the mice immunized with p135–153 or overlapping peptides developed CNS autoimmunity are reminiscent of T-cell recognition of interphotoreceptor retinoid-binding protein (IRBP), a multi-determinant uveitogenic autoantigen (28) expressed in the thymus that possesses an epitope that is subject to *Aire*-dependent negative selection and another that is not subject to negative selection (29, 30). Our demonstration that both pathogenic T-cell and TCR repertoire selection in AQP4^{-/-} and WT mice are distinct underscores the importance of investigating how thymic negative selection,

and possibly *Aire* or *Fezf2*, may influence differentiation of AQP4-specific T cells in ATCA and NMO.

Of note, tolerance to MOG and other myelin autoantigens is not governed by the same mechanisms (31, 32). Immunization of WT H-2^b mice with MOG p35–55 provides T cells that are reactive to that self-antigen. When polarized to Th17, adoptive transfer of those T cells induces extensive myelitis and optic neuritis (Figs. 3 and 4) (33). Of particular interest, a form of neuroinflammation resembling NMO that is negative for antibody to AQP4, seen in a small proportion of clinical cases of NMO, is driven by immunity to MOG (17).

In this report, we have established a role for T cells in ATCA. We have identified multiple pathogenic AQP4 T-cell epitopes and demonstrated how those AQP4-specific T cells can enter the CNS to initiate clinical and histologic CNS disease. However, we have not created NMO in mice. Both cellular and humoral immunity contribute to NMO pathogenesis. In this regard, AQP4-specific IgG (5, 6), which is T-cell-dependent, has a key role in the effector phase of NMO. By identification and characterization of pathogenic AQP4-specific T cells, we have established a foundation to study how cellular and humoral immunity cooperate in ATCA, which should provide further insight regarding the immune pathogenesis of NMO.

Materials and Methods

Mice. C57BL/6 (H-2^b) and SJL/J (H-2^s) female mice, 8 wk of age, were purchased from the Jackson Laboratories. C57BL/6 AQP4^{-/-} mice were provided by A. Verkman, University of California, San Francisco; B-cell-deficient (J μ T) mice by K. Rajewsky, Harvard, Cambridge, MA; and SJL/J RAG2^{-/-} mice by H. Waldner, Pennsylvania State University, University Park, PA. Mice were housed under specific pathogen-free conditions at UCSF Laboratory Animal Research Center. All studies were approved by the UCSF Institutional Animal Care and Use Committee.

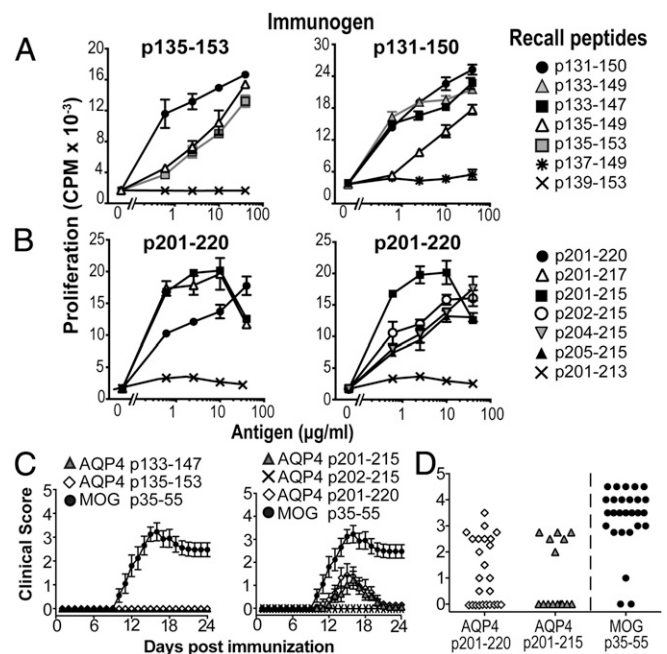


Fig. 6. Fine specificity characterization of AQP4-specific T cells reveals peptide within p201–220 that induces ATCA. Wild-type mice (two per group) were immunized with (A) AQP4 p135–151 or p131–150 or (B) p201–220 and evaluated for recall to nested peptides within these determinants. Proliferation was measured by ³H-thymidine incorporation (mean \pm SEM, representative of three experiments). (C) WT mice were immunized with AQP4 peptides or MOG p35–55 for induction of CNS autoimmune disease. Results represent mean (\pm SEM) group clinical scores; $n = 10$ per group. (D) Graph represents maximal clinical scores for individual WT mice shown in C. Data are a composite of five independent experiments.

Antigens. Genemed Synthesis provided all peptides.

Proliferation Assays. AQP4^{-/-} or WT mice were immunized with 100 μ g of AQP4 or MOG peptide in CFA. Lymph nodes were harvested on day 11 and cultured at 2×10^5 per well with peptide for 72 h. The incorporation of ³H-thymidine is measured in triplicate wells.

TCR V β Analysis. AQP4^{-/-} and WT mice were immunized with AQP4 or MOG peptides. Lymph node cells were isolated 11 d later and cultured with 20 μ g/mL antigen for 10–14 d. TCR V β utilization was analyzed by FACS using the TCR V β Screen Kit (BD Bioscience).

Flow Cytometry. Cell surface staining was performed with antibodies specific for CD3, CD4, CD8, B220, CD11b, CD11c, Ly6G, and annexin V (eBioscience). Proinflammatory T-cell polarization was evaluated by *in vitro* stimulation with 50 ng/mL PMA (Sigma-Aldrich) and 1 μ g/mL ionomycin (Sigma-Aldrich) in the presence of 1 μ g/mL BD GolgiStop (BD Bioscience) for 4 h. Intracellular cytokine staining (ICS) was conducted with antibodies specific for IFN- γ , IL-17, CD25, and Foxp3.

CNS Autoimmune Disease Induction and Analysis. Mice were immunized s.c. with 100 μ g of AQP4 or MOG peptide in CFA containing 400 μ g *Mycobacterium tuberculosis* H37Ra (Difco Laboratories). Mice received 200 ng *B. pertussis* toxin (Ptx) (List Biological) by i.p. injection on days 0 and 2. For adoptive induction of ATCA, mice were immunized with 100 μ g AQP4 or MOG peptides in CFA. After 11 d, lymph node cells were cultured with 15 μ g/mL antigen for 3 d under Th17 (20 ng/mL IL-23 and 10 ng/mL IL-6) or Th1 (10 ng/mL IL-12) polarizing conditions. We injected i.v. 2×10^7 cells into naive recipients. At day 0 and 2, mice received Ptx. When stated, donor T cells were labeled with 10 μ M carboxyfluorescein diacetate succinimidyl ester (CFSE) (Invitrogen). Clinical scores were as follows: 0, no disease; 1, tail tone loss; 2, impaired righting; 3, severe paraparesis or paraplegia; 4, quadraparesis; 5, moribund or death.

Histopathology. Brain, spinal cord, optic nerve, kidney, and muscle tissue samples were fixed in 10% (vol/vol) neutral-buffered formalin, paraffin-embedded, sectioned, and stained with Luxol fast blue (LFB)/H&E. Meningeal and parenchymal inflammatory lesions and areas of demyelination were

assessed in a blinded manner as previously described (34). Avidin-biotin immunohistochemical staining was performed with anti-CD3, anti-CD45R (B220), and anti-Iba1. Axonal loss was assessed using Bielschowsky silver impregnation.

In Situ Whole-Mount Immunofluorescence Microscopy. Whole-mount immunostaining was performed on retinas and CNS tissues, which were harvested at peak disease and at the end of the experiment. RGCs were stained with Brn3a and quantified with a custom-made macro on ImageJ (1.51, NIH). Donor CNS infiltrating T cells were identified by CFSE and CD3; infiltrating monocyte/macrophage and resident microglia were identified by Iba1. Images were collected using a Zeiss LSM-700 confocal system equipped with Zen software and processed in ImageJ.

In Vivo Retinal Imaging. Spectral domain (SD) OCT retinal imaging was performed using Spectralis (Heidelberg Engineering) with the TruTrack eye-tracker to avoid motion artifacts. Mice were anesthetized and eyes dilated. Volume OCT scans were performed throughout the disease. Scans consisted of 25 B-Scans recorded in high-resolution mode and rasterized from 30 averaged A-Scans. After automated segmentation by Heidelberg Eye Explorer software and blind manual correction of segmentation errors, average thickness of IRL (defined as retinal nerve fiber layer, ganglion cell layer, and inner plexiform layer) (35) was measured using a ring-shaped grid. The central sector, corresponding to the optic nerve head, was excluded. Differences were analyzed using generalized estimating equations with an exchangeable correlation matrix and adjustments for intrasubject intereye correlations.

Statistical Analysis. Data are presented as mean \pm SE of mean (SEM). Analysis was performed using multiple *t* tests, and significance was determined with the Holm-Sidak method, unless otherwise stated. *P* values are designated as follows: **P* \leq 0.5, ***P* \leq 0.01, ****P* \leq 0.001.

ACKNOWLEDGMENTS. Support was provided to S.S.Z. by National Institute of Health Grant RO1 AI073737; National Multiple Sclerosis Society (NMSS) Grants RG 4768, RG 5179, and RG 5180; the Guthy Jackson Charitable Foundation; and the Maisin Foundation.

- Hardy TA, et al. (2016) Atypical inflammatory demyelinating syndromes of the CNS. *Lancet Neurol* 15(9):967–981.
- Lucchinetti CF, et al. (2014) The pathology of an autoimmune astrocytopathy: Lessons learned from neuromyelitis optica. *Brain Pathol* 24(1):83–97.
- Zekeridou A, Lennon VA (2015) Aquaporin-4 autoimmunity. *Neurol Neuroimmunol Neuroinflamm* 2(4):e110.
- Nurieva RI, Chung Y (2010) Understanding the development and function of T follicular helper cells. *Cell Mol Immunol* 7(3):190–197.
- Bennett JL, et al. (2009) Intrathecal pathogenic anti-aquaporin-4 antibodies in early neuromyelitis optica. *Ann Neurol* 66(5):617–629.
- Bradl M, et al. (2009) Neuromyelitis optica: Pathogenicity of patient immunoglobulin *in vivo*. *Ann Neurol* 66(5):630–643.
- Brum DG, et al. (2010) HLA-DRB association in neuromyelitis optica is different from that observed in multiple sclerosis. *Mult Scler* 16(1):21–29.
- Varrin-Doyer M, et al. (2012) Aquaporin 4-specific T cells in neuromyelitis optica exhibit a Th17 bias and recognize Clostridium ABC transporter. *Ann Neurol* 72(1):53–64.
- Vaknin-Dembinsky A, et al. (2012) T-cell reactivity against AQP4 in neuromyelitis optica. *Neurology* 79(9):945–946.
- Nelson PA, et al. (2010) Immunodominant T cell determinants of aquaporin-4, the autoantigen associated with neuromyelitis optica. *PLoS One* 5(11):e15050.
- Kalluri SR, et al. (2011) Functional characterization of aquaporin-4 specific T cells: Towards a model for neuromyelitis optica. *PLoS One* 6(1):e16083.
- Pohl M, et al. (2011) Pathogenic T cell responses against aquaporin 4. *Acta Neuropathol* 122(1):21–34.
- Zeka B, et al. (2015) Highly encephalitogenic aquaporin 4-specific T cells and NMO-IgG jointly orchestrate lesion location and tissue damage in the CNS. *Acta Neuropathol* 130(6):783–798.
- Jones MV, Huang H, Calabresi PA, Levy M (2015) Pathogenic aquaporin-4 reactive T cells are sufficient to induce mouse model of neuromyelitis optica. *Acta Neuropathol Commun* 3:28.
- Vita R, et al. (2015) The immune epitope database (IEDB) 3.0. *Nucleic Acids Res* 43(Database issue):D405–D412.
- Shetty A, et al. (2014) Immunodominant T-cell epitopes of MOG reside in its transmembrane and cytoplasmic domains in EAE. *Neurol Neuroimmunol Neuroinflamm* 1(2):e22.
- Zamvil SS, Slavin AJ (2015) Does MOG Ig-positive AQP4-seronegative opticospinal inflammatory disease justify a diagnosis of NMO spectrum disorder? *Neurol Neuroimmunol Neuroinflamm* 2(1):e62.
- Matsushita T, et al. (2013) Characteristic cerebrospinal fluid cytokine/chemokine profiles in neuromyelitis optica, relapsing remitting or primary progressive multiple sclerosis. *PLoS One* 8(4):e61835.
- Mobasheri A, et al. (2007) Distribution of the AQP4 water channel in normal human tissues: Protein and tissue microarrays reveal expression in several new anatomical locations, including the prostate gland and seminal vesicles. *Channels (Austin)* 1(1):29–38.
- Fernandes DB, et al. (2013) Evaluation of inner retinal layers in patients with multiple sclerosis or neuromyelitis optica using optical coherence tomography. *Ophthalmology* 120(2):387–394.
- Zamvil SS, et al. (1986) T-cell epitope of the autoantigen myelin basic protein that induces encephalomyelitis. *Nature* 324(6094):258–260.
- Levin MH, Bennett JL, Verkman AS (2013) Optic neuritis in neuromyelitis optica. *Prog Retin Eye Res* 36:159–171.
- Chi Y, et al. (2011) Novel role of aquaporin-4 in CD4+ CD25+ T regulatory cell development and severity of Parkinson's disease. *Aging Cell* 10(3):368–382.
- Anderson MS, et al. (2002) Projection of an immunological self shadow within the thymus by the Aire protein. *Science* 298(5597):1395–1401.
- Takaba H, et al. (2015) Fezf2 orchestrates a thymic program of self-antigen expression for immune tolerance. *Cell* 163(4):975–987.
- Derbinski J, et al. (2005) Promiscuous gene expression in thymic epithelial cells is regulated at multiple levels. *J Exp Med* 202(1):33–45.
- Hubert FX, et al. (2011) Aire regulates the transfer of antigen from mTECs to dendritic cells for induction of thymic tolerance. *Blood* 118(9):2462–2472.
- Caspi RR (2010) A look at autoimmunity and inflammation in the eye. *J Clin Invest* 120(9):3073–3083.
- DeVoss J, et al. (2006) Spontaneous autoimmunity prevented by thymic expression of a single self-antigen. *J Exp Med* 203(12):2727–2735.
- Taniguchi RT, et al. (2012) Detection of an autoreactive T-cell population within the polyclonal repertoire that undergoes distinct autoimmune regulator (Aire)-mediated selection. *Proc Natl Acad Sci USA* 109(20):7847–7852.
- Delarasse C, et al. (2003) Myelin/oligodendrocyte glycoprotein-deficient (MOG-deficient) mice reveal lack of immune tolerance to MOG in wild-type mice. *J Clin Invest* 112(4):544–553.
- Zamvil S, et al. (1985) T-cell clones specific for myelin basic protein induce chronic relapsing paralysis and demyelination. *Nature* 317(6035):355–358.
- Herges K, et al. (2012) Protective effect of an elastase inhibitor in a neuromyelitis optica-like disease driven by a peptide of myelin oligodendroglial glycoprotein. *Mult Scler* 18(4):398–408.
- Molnarfi N, et al. (2013) MHC class II-dependent B cell APC function is required for induction of CNS autoimmunity independent of myelin-specific antibodies. *J Exp Med* 210(13):2921–2937.
- Cruz-Herranz A, et al.; IMSVISUAL consortium (2016) The APOSTEL recommendations for reporting quantitative optical coherence tomography studies. *Neurology* 86(24):2303–2309.

Supporting Information

Sagan et al. 10.1073/pnas.1617859114

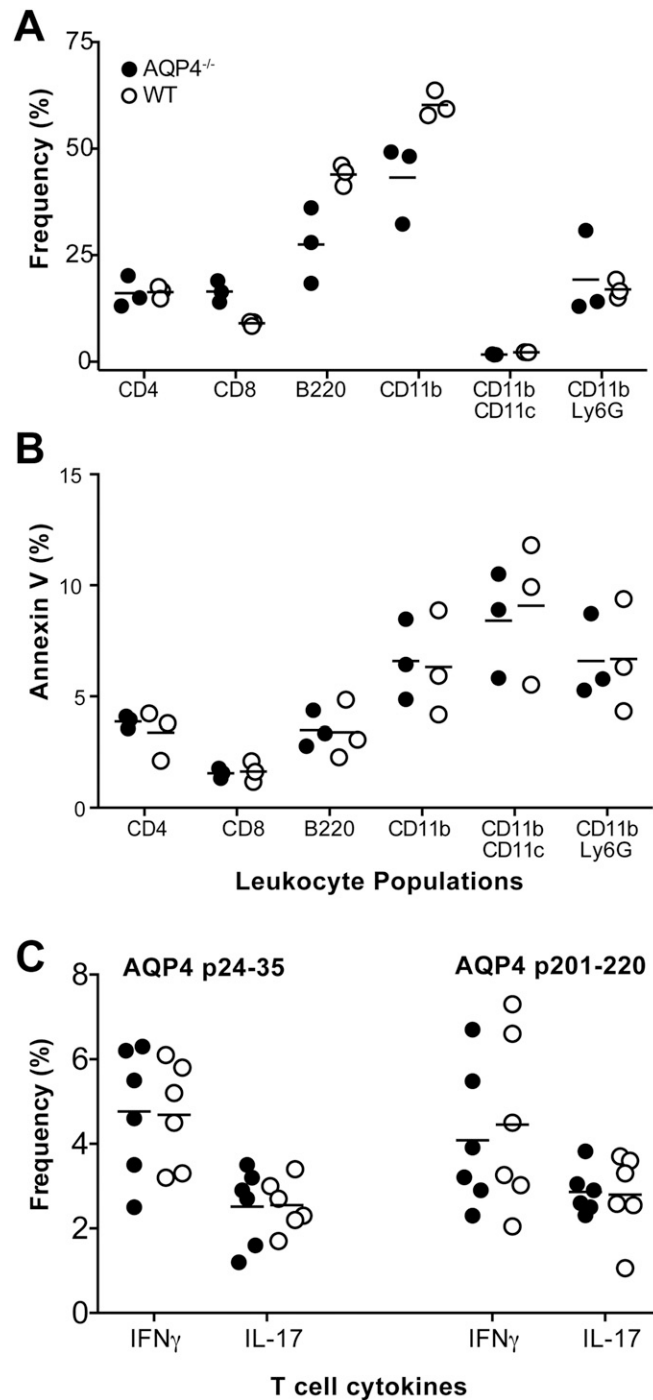


Fig. S1. Flow cytometry analysis of leukocyte populations, apoptosis, and T-cell cytokines from splenocytes of AQP4^{-/-} and WT mice primed with AQP4 peptides. (A) AQP4^{-/-} and WT mice were immunized with AQP4 p201–220. At day 11, spleens were harvested and peripheral leukocyte subsets were analyzed by flow cytometry. The mean is represented for three mice per group. (B) Annexin V staining from leukocyte subsets of AQP4^{-/-} and WT primed with AQP4 p201–220 is compared. The mean is represented for three mice per group. (C) AQP4^{-/-} and WT mice were immunized with AQP4 p24–35 and p201–220, and the IFN γ and IL-17 secretion from CD4⁺ T cells was analyzed by flow cytometry. Data represented are a composite of four experiments.

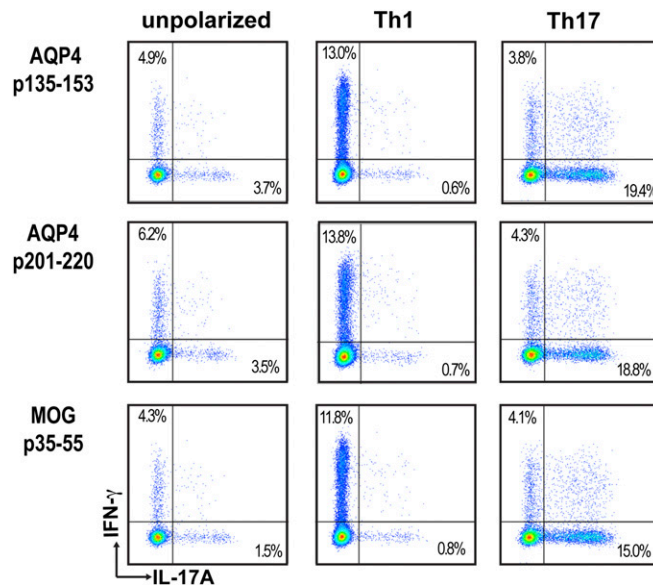


Fig. S2. Flow cytometry analysis of Th1- and Th17-polarized AQP4-specific donor T cells. AQP4^{-/-} mice were immunized with 100 μ g of AQP4 p135–153 or p201–220. WT mice were immunized with MOG p35–55. Lymph nodes were harvested 11 d later and cultured with antigen under Th1 (10 ng/mL IL-12) or Th17 (20 ng/mL IL-23 and 10 ng/mL IL-6) polarizing conditions. As a control, cells were cultured without cytokines and designated as unpolarized. IFN- γ - and IL-17A-producing cells were analyzed by intracellular staining. The data are representative of eight experiments.

Table S1. AQP4 T-cell epitopes identified from analysis of WT C57BL/6 and SJL/J mice were not pathogenic

Strain, disease model, and antigen	Incidence	Mean maximal clinical score*	Mean number of foci (\pm SEM)*		
			Meninges	Parenchyma	Total
C57BL/6					
Direct immunization ^{†,‡}					
CFA only	0/9	0	0	0	0
AQP4 p24–35	0/12	0	0	0	0
AQP4 p91–110	0/12	0	0	0	0
AQP4 p261–280	0/12	0	0	0	0
MOG p35–55	6/6	2.9 (\pm 0.7)	68.5 (\pm 14.6)	110.2 (\pm 22.2)	177.5 (\pm 34.8)
Adoptive transfer [§]					
AQP4 p24–35	0/6	0	0	0	0
AQP4 p24–35 (Th1)	0/4	0	0	0	0
AQP4 p24–35 (Th17)	0/7	0	0	0	0
MOG p35–55 (Th1)	4/4	2.8 (\pm 0.5)	148.0 (\pm 16.1)	148.8 (\pm 20.7)	296.5 (\pm 36.3)
MOG p35–55 (Th17)	5/5	3.0 (\pm 0.4)	87.2 (\pm 26.2)	79.4 (\pm 27.5)	166.6 (\pm 52.7)
SJL/J					
Direct immunization [†]					
CFA only	0/5	0	0	0	0
AQP4 p23–35	0/5	0	0	0	0
AQP4 p16–30	0/5	0	0	0	0
AQP4 p101–119	0/5	0	0	0	0
PLP p139–151	5/5	2.8 (\pm 0.4)	76.5 (\pm 22.5)	72.5 (\pm 0.3)	148.5 (\pm 22.5)
Adoptive transfer [§]					
AQP4 p23–35 (Th1)	0/5	0	0	0	0
AQP4 p23–35 (Th17)	0/5	0	0	0	0
PLP p139–151 (Th1)	4/4	3.2 (\pm 0.6)	122.8 (\pm 26.3)	157.8 (\pm 27.3)	280.5 (\pm 53.4)
PLP p139–151 (Th17)	4/4	3.1 (\pm 0.5)	144.0 (\pm 21.9)	189.0 (\pm 23.7)	388.0 (\pm 45.3)

*All values are shown as mean (\pm SEM).

[†]Direct immunization with 100 μ g Ag in CFA.

[‡]C57BL/6 (not SJL/J) mice received PTX on day 0 and 2.

[§]Donor T cells (2×10^7), polarized to Th1 using 10 ng/mL IL-12 or to Th17 using 20 ng/mL IL-23 and 10 ng/mL IL-6.

Table S2. Adoptive transfer of AQP4 p23–35 Th17 cells into pretreated SJL/J recipients

Donor T cells*	Pretreatment of recipient mice	Incidence	Mean maximal clinical score [†]	Mean number of foci (±SEM)		
				Meninges	Parenchyma	Total
AQP4 p23–35 (Th17)	None	0/5	0	10 (±4.7)	9.4 (±7.5)	19.4 (±11.9)
	Ptx [‡]	0/5	0	3.2 (±0.8)	12.0 (±1.8)	14.8 (±2.2)
	Irradiation [§]	0/5	0	165 (±25.4)	191.2 (±35.3)	350.2 (±54.6)
	Ptx [‡] and irradiation [§]	0/5	0	25.2 (±6.7)	51.0 (±10.7)	76.2 (±17.2)
	RAG2 ^{-/-} recipients	0/9	0	3.4 (±2.0)	9.3 (±2.7)	12.8 (±3.4)
PLP p139–151 (Th17)	None	5/5	3.2 (±0.6)	236.8 (±16.5)	255 (±12.7)	481.8 (±8.0)

*Donor T cells (2×10^7) were polarized to Th17 using 20 ng/mL IL-23 and 10 ng/mL IL-6.

[†]All values are shown as mean (±SEM).

[‡]Mice received 200 ng Ptx on days 0 and 2 posttransfer.

[§]600 rad given.

Table S3. Statistical analysis for CNS infiltrates from the adoptive transfer of AQP4-primed T cells from AQP4^{-/-} mice into WT recipients

Donor T cells*	Meninges [†]	P value [‡]	Parenchyma [†]	P value [‡]	Total [†]	P value [‡]
Th1 polarized donor cells						
MOG p35–55	115 (±10)	—	101 (±21)	—	216 (±11)	—
AQP4 p135–153	25 (±9)	<0.0001	12 (±2)	0.0282	37 (±10)	0.0008
AQP4 p201–220	55 (±15)	0.0026	17 (±5)	0.0009	72 (±19)	<0.0001
Th17 polarized donor cells						
MOG p35–55	151 (±20)	—	163 (±13)	—	314 (±33)	—
AQP4 p135–153	101 (±18)	0.1035	38 (±10)	0.0001	139 (±19)	0.0032
AQP4 p201–220	135 (±15)	0.4527	82 (±17)	0.0031	206 (±28)	0.0418

*Donor-primed T cells were cultured in vitro in Th1 (10 ng/mL IL-12) or Th17 (20 ng/mL IL-23 and 10 ng/mL IL-6) polarizing conditions for 72 h. We administered 2×10^7 donor T cells i.v. to recipient mice.

[†]All values are shown as mean (±SEM); $n = 5$ per group.

[‡]The CNS infiltrates are compared with the MOG control using an unpaired, two-tailed t test with Welch's correction for unequal SDs.

Table S4. Inflammation was present in the CNS but not in kidneys or skeletal muscle of recipients of AQP4-primed T cells

Donor T cells*	Incidence of ATCA	Mean clinical score [†]	CNS inflammation	Nephritis	Myositis
AQP4 p135–153, Th1	5/5	1.2 (±0.2)	5/5	0/5	0/5
AQP4 p135–153, Th17	5/5	2.4 (±0.2)	5/5	0/5	0/5
AQP4 p201–220, Th1	5/5	1.3 (±0.2)	5/5	0/5	0/5
AQP4 p201–220, Th17	5/5	2.4 (±0.3)	5/5	0/5	0/5

*Donor AQP4^{-/-} T cells (2×10^7), polarized to Th1 or Th17, were administered i.v. to recipient WT mice.

[†]All values are shown as mean (±SEM).

Table S5. Donor AQP4-primed T cells from AQP4^{-/-} mice induce clinical CNS autoimmunity in WT recipients

Donor T cells*	Donor	Recipient	Incidence	Onset, d [†]	Mean maximal clinical score [†]
AQP4 p135–153	Th17	AQP4 ^{-/-} WT	6/6	6.8 (±0.4)	2.6 (±0.2)
AQP4 p135–149	Th17	AQP4 ^{-/-} WT	6/6	9.2 (±0.5)	2.4 (±0.2)
AQP4 p201–220	Th17	AQP4 ^{-/-} WT	5/5	7.2 (±0.4)	2.7 (±0.2)
AQP4 p201–215	Th17	AQP4 ^{-/-} WT	4/5	6.8 (±0.3)	2.4 (±0.4)
MOG p35–55	Th17	WT	5/5	7.0 (±0.3)	3.2 (±0.2)

*Donor T cells (2×10^7) were polarized to Th17 using 20 ng/mL IL-23 and 10 ng/mL IL-6.

[†]All values are shown as mean (±SEM).



Movie S1. AQP4 p135–153-specific T cells cause paralysis in recipient WT mouse. Th17-polarized AQP4 p135–153-specific T cells from AQP4^{-/-} mice were transferred into WT recipients. Shown is a representative recipient mouse with severe ATCA.

[Movie S1](#)